Minimum energy conformation of ortho-xylene in its ground and first excited electronic states

R. Disselkamp and E. R. BernsteinJeffrey I. Seeman and Henry V. Secor

Minimum energy conformation of *ortho*-xylene in its ground and first excited electronic states

R. Disselkamp and E. R. Bernstein
Colorado State University, Chemistry Department, Fort Collins, Colorado 80523

Jeffrey I. Seeman and Henry V. Secor
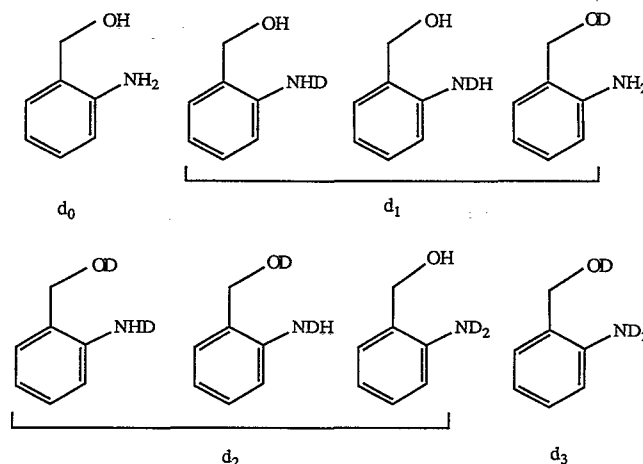*Philip Morris Research Center, P. O. Box 26583, Richmond, Virginia 23261*

The geometry of *ortho*-xylene is studied through supersonic jet cooling and one color mass resolved excitation spectroscopy. By examining the $S_1 \leftarrow S_0$ transition origin region of various (d_0-d_2) methyl deuterated *o*-xylene species, the conformation of the two methyl groups in S_0 and S_1 can be determined. A comparison between the predicted and experimentally observed number and intensity of origin features for the various partially deuterated *o*-xylenes shows that two highly symmetric methyl group structures are possible, each structure having C_{2V} point group symmetry—the antiplanar conformation (A1), in which $\tau_1(C_2-C_1-C_\alpha-H_\alpha)$ $=180°$; $\tau_2(C_1-C_2-C_{\alpha'}-H_{\alpha'})=180°$; and the *syn*, planar conformation (A2) in which $\tau_1=\tau_2$ $=0°$. The experimentally determined structures are consistent with *ab initio* calculations and microwave studies which predict the anticonformation to be most stable. Spectroscopic data, in conjunction with further *ab initio* calculations, are used to investigate the ground and excited state potential energy surfaces. In addition, a repulsive, intramolecular, nonbonded interaction between the two methyl groups is identified through an empirical potential energy calculation to be the most important interaction defining the lowest energy structure.

I. INTRODUCTION

A detailed understanding of chemical properties, bonding, and reactions rests on a knowledge of molecular structures and, more generally, on a knowledge of molecular potential energy surfaces. Such information typically comes from nuclear magnetic resonance (NMR), microwave, vibration–rotation, and electronic spectroscopies. In this work, we report a novel implementation of relatively low-resolution optical spectroscopy of isotopically substituted compounds which can lead to structural information by revealing the local symmetry in the vicinity of isotopic substitution. A central idea of this work is that each isomer of a given molecule will possess unique bonding properties such that its optical absorption spectrum, in particular, its $S_1 \leftarrow S_0$ 0_0^0 transition, which reflects zero point vibrational energy changes between these electronic states, will be unique and distinct from that of other isomers.

For example, the spectra of 2-aminobenzyl alcohol isomers $-d_0$, d_1, d_2, and d_3 as indicated in scheme I, give rise to a total of one, three, three, and one origin transitions,[1] respectively, which indicates an inequivalence of the two N–H bonds in this molecule. Such an experimental observation requires that the single most stable structural conformation observed for this molecule maintain symmetry inequivalence of the two N–H bonds. Indeed, semiempirical calculations on 2-aminobenzyl alcohol indicate that the CH_2OH sidechain substituent lies perpendicular to the aromatic ring and that the amino group lies nearly in the plane of the aromatic ring, consistent with the deuteration experimental results.

Scheme I

d_0 d_1

d_2 d_3

Here we examine the $S_1 \leftarrow S_0$ origin spectra of isotopomers of partially methyl deuterated *o*-xylenes **1–4**. The effects of deuteration will be used to determine the symmetry species of the two methyl groups in a similar manner to that described above for the 2-aminobenzyl alcohol system. Various methyl group orientations of different symmetry types are illustrated in Fig. 1. In addition, Table I lists the expected number of origin features and intensities (statistical weights) for the structures of Fig. 1 corresponding to a particular deuteration type **1–4**. For example, the type A structures of Fig. 1 each have two energetically and symmetry distinct methyl hydrogen sites in the ratio of 4:2.
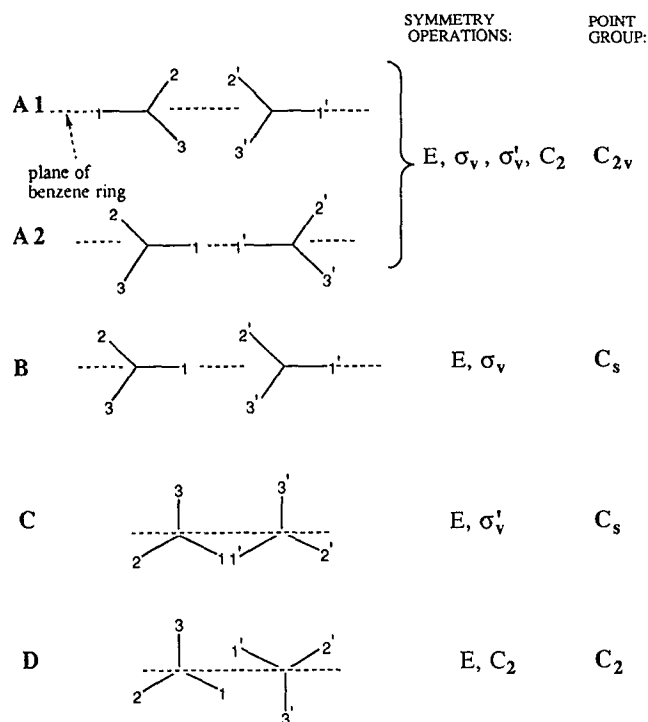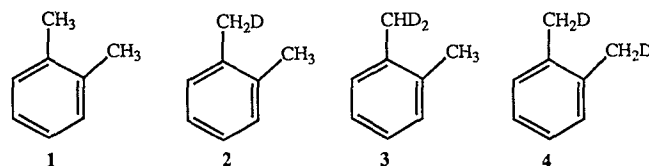
CONFORMATIONS OF METHYL GROUPS IN O-XYLENE

| | SYMMETRY OPERATIONS: | POINT GROUP: |

FIG. 1. Various methyl group structures in *o*-xylene are shown with their respective symmetry elements and molecular point group.

The symmetric d_2 deuteration of these structures would then lead to four unique isotopomers (see Fig. 1). These results are listed in the final column of Table I under the type A structures. To summarize, different hypothetical ground state energy minima (i.e., stable orientations of the methyl groups) generate different numbers of energetically unique isotopomers which in turn correspond one to one with distinct optical transitions for the various isotopologues of *o*-xylenes 1–4.

As demonstrated previously,[2] the combined techniques of supersonic expansion cooling, mass resolved excitation spectroscopy (MRES), chemical and isotopic substitution, in conjunction with symmetry considerations such as those mentioned above, can often lead to a unique determination of molecular structure. This experimental approach generates a characteristic set of optical transitions (0^0_0 etc.) for each unique geometric conformation of interest. Hence, one can often make a one-to-one correspondence between the spectra and the molecular conformations.

Previous experimental studies of *o*-xylene[2(a),3–10] show that relatively large barriers to internal rotation of the methyl groups exist in the ground (~ 600 cm^{-1}) and first excited (~ 150 cm^{-1}) electronic states. Much of this experimental data has been fit to a combination of effective Hamiltonian parameters including individual threefold and sixfold potential energy terms for each methyl group, individual kinetic energy contributions from each methyl group, and coupling kinetic and potential energy terms between the two methyl groups. Most of these investigations of the methyl rotor potential surface, however, could not identify unambiguously a minimum energy structure. Two independent studies, one experimental[8] and the other theoretical,[11] both suggest the same minimum energy conformation of *o*-xylene, that being structure A1 of Fig. 1. In our discussion, here we will present unique experimental, and more detailed theoretical results which support this assignment for both the ground and first excited singlet electronic states.

II. EXPERIMENTAL PROCEDURES

The $S_1 \leftarrow S_0$ origin region of *o*-xylene is studied using mass resolved excitation spectroscopy, the details of which are described previously.[12] Spectra are collected using a

TABLE I. *O*-xylene inequivalent conformers and statistical weights.

	Structure	d_0	d_1	d_2 (asymmetric)	d_2 (symmetric)
A1		1 1	2 2:1	2 2:1	4 4:2:2:1
A2					
B		1 1	4 2:2:1:1	4 2:2:2:1	4 2:2:2:1
C		1 1	3 1:1:1	3 1:1:1	6 2:2:2:1:1:1
D		1 1	3 1:1:1	3 1:1:1	6 2:2:2:1:1:1

one color-two photon resonance enhanced ionization technique and the ions are subsequently mass selected. A cold beam of molecules (translational temperature < 1 K) is generated by skimming an expansion from a Jordan pulsed valve operating at 10 Hz. The output from a Spectra Physics DCR III Nd^{+3}/YAG pumped dye laser (LDS 698 dye) is frequency doubled and mixed with residual 1.064 μm radiation and then focused into the vacuum chamber between a pair of ion extraction plates for a time-of-flight mass spectrometer. Ions are formed by scanning the laser energy and exciting $S_1 \leftarrow S_0$ resonances which then undergo ionization by absorption of a second photon. The resulting ions are accelerated and focused onto a Galileo Electro-Optics multichannel plate detector. The current output from this detector is analyzed using a boxcar averager. Ten laser pulses are averaged per data point collected. Helium is employed as the expansion gas at a pressure of 40 psig and all samples are kept at room temperature prior to their expansion.

Details of our synthesis of the deuterated xylenes will be reported elsewhere. Note, however, that the synthesis of deuteration types **2** and **4** have been reported previously.[13]

III. RESULTS AND DISCUSSION

A. Experiment

The spectra of various methyl deuterated ($-d_0$, $-d_1$, $-d_2$) *o*-xylenes are presented in Fig. 2. The *o*-xylene $S_1 \leftarrow S_0$ 0_0^0 transition, which is arbitrarily set to zero wave numbers in Fig. 2(a), occurs at 37 313 cm^{-1}. The smaller features indicated by asterisks in Fig. 2 arise from saturated, intense signals in lower mass channels ringing into higher mass channels. Three important observations about these spectra will be discussed—the number of origins identified in each isotopically substituted *o*-xylene, the relative intensities of the features, and the relative energy of each feature. The experimental data will be used to identify the orientation of the methyl groups with respect to the aromatic ring and to infer S_1 geometry from the predicted S_0 geometry through Franck–Condon factor arguments.

The spectrum of nondeuterated *o*-xylene [Fig. 2(a)] shows one feature—this is consistent with a single stable conformation of *o*-xylene in S_0 and S_1 for which any one of the proposed model structures A–D presented in Fig. 1 and Table I is acceptable. The MRES of *o*-xylene-α-d_1 (**2**) has two features with a 2:1 intensity ratio. This spectroscopic result is uniquely consistent with the two structures having C_{2V} symmetry labeled A1 and A2 in Fig. 1. If the C_{2V} structures are assumed to be correct, one further expects that the asymmetrical d_2 [CHD_2, CH_3 (deuteration type 3)] will yield two features with a 2:1 intensity ratio and that the symmetrical d_2 [CH_2D, CH_2D (deuteration type 4)] will have four features with a 4:2:2:1 intensity ratio. These expectations prove correct as can be seen from Fig. 2. All other structures for partially methyl deuterated *o*-xylenes would generate more spectroscopic features than those observed and displayed in Fig. 2. Because of the uniqueness of the predicted and observed relative peak intensities, we are able to assign two specific deuterated
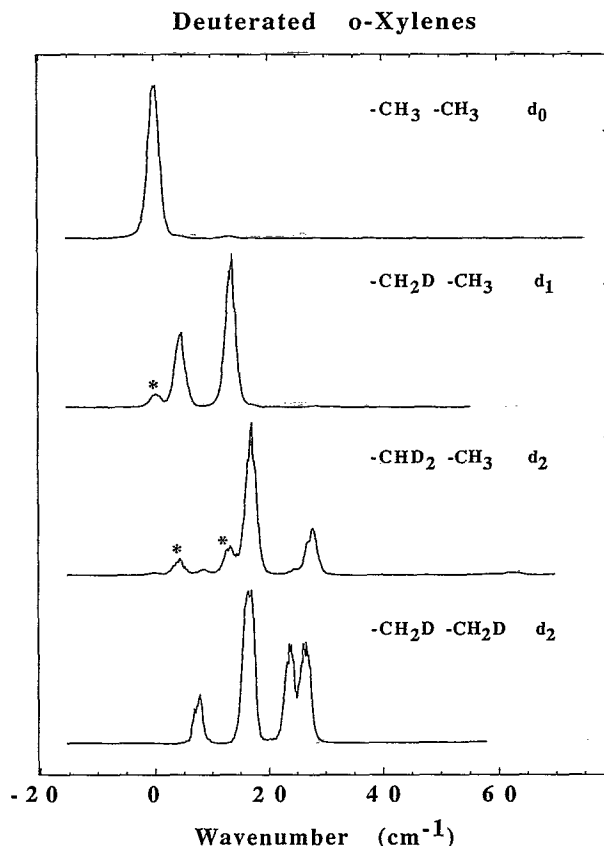

Deuterated   o-Xylenes

FIG. 2. The mass resolved excitation spectra (MRES) of methyl deuterated *o*-xylenes are plotted relative to the undeuterated (d_0) origin located at 37 313 cm^{-1}. The asterisks indicate intense features from the lower mass channel contributing to the spectrum.

structures to the observed features. The conformational energy difference between this antiplanar structure and the *syn* planar structure will be discussed in the next section.

Since the relative intensities of the observed features at the $S_1 \leftarrow S_0$ 0_0^0 transition of the isotopomers reflect a statistical isotope distribution, and since all of the Franck–Condon transition intensity is retained at the origin of each isotopolog,[3(a)] the methyl group structures in the S_0 and S_1 states have the same single stable conformation. This is a good assumption because the S_0 and S_1 vibrations are only perturbed slightly by the deuteration, and only conformer 0_0^0 transitions are observed. *Ab initio* calculations discussed in the next section support this conclusion.

B. *Ab initio* calculations and potential energy surfaces for S_0

The calculational results of conformational energy presented here are obtained using a GAUSSIAN 88 molecular orbital program[14] operating on an IBM RISC/6000 computer system. Hartree–Fock calculations are performed without symmetry on the ground state structures of Fig. 1 by performing a geometry optimization of all bond distances and angles except the six dihedral angles which uniquely specify the appropriate methyl group structure of interest. This procedure is implemented using three differ-

TABLE II. *Ab initio* RHF relative in (cm^{-1}) and absolute (in atomic units) energies[a] for the various conformations of o-xylene.

	Structure	STO-3G	3-21G*	6-31G**
A1		0.0 ($-305.059\ 102\ 9$)	0.0 ($-307.060\ 493\ 8$)	0.0 ($-308.792\ 912\ 4$)
A2		965.0	1024.0	1047.0
B		407.0	472.0	463.0
C		528.0	581.0	578.0
D		416.0	494.0	466.0

[a]One atomic unit $=2.195\times10^5$ cm^{-1}.

ent basis sets—the minimal basis Slater-type orbital (STO)-3G, and the split–valence plus polarization basis sets 3-21G* and 6-31G**. The STO-3G optimized geometry for each structure is used as the initial input for geometry optimizations involving the larger basis sets. The results of these calculations are listed in Table II. The calculated energy of the minimum energy structure A1 has been set equal to zero for each basis set and the relative energies of the other structures are expressed in wave numbers. Structure A1 is calculated to be the most stable within each basis set. The relative energy differences between structures are roughly constant as the basis set for the Hartree–Fock calculation is expanded from STO-3G to 6-31G**. The consistency of these results is encouraging and adds support to the previous minimal basis set molecular orbital (MO) calculations.[11] Throughout these calculations, the aromatic ring retains a nearly planar structure.

Insight into preferred internal rotational motion of the methyl groups can be gained by examining the conformational energies displayed in Table II. Two extremes in methyl group internal rotation are coupled methyl group rotational motion in either a conrotary or disrotary fashion and a single independent methyl group rotation. If the molecule is in its minimum energy structure A1, coupled methyl rotor motion leads to structure A2 at approximately 1000 cm^{-1}, and independent single rotor motion leads to the geared structure B at roughly 450 cm^{-1} (in S_0). Since the experimentally determined values of methyl rotor barriers range anywhere from 500–700 cm^{-1},[2(a),3–10] the independent rotation of a single methyl group might be a low energy path to interconversion between conformers.

Both the above restricted Hartree–Fock (RHF) calculation and a qualitative (6-12-1) Lennard-Jones Coulomb intramolecular nonbonded potential energy calculation can be used in an attempt to understand why structure A1 is indeed the minimum energy structure. Figure 3 illustrates schematically how the RHF calculated in-plane angle φ varies for the different structures of Fig. 1. In this figure, $\varphi=0$ (the two dashed lines) corresponds to both $\varphi(C_2-C_1-C_\alpha)=\varphi(C_1-C_2-C_{\alpha'})=120°$. A strong correlation exists between the magnitude of φ and the relative energies listed in Table II. Since larger values of φ correspond to less

stable structures, a repulsive steric interaction is likely to be responsible for determining the methyl group orientations. To test this supposition, the methyl group–methyl group interaction energy for the various structures of Fig. 1 is calculated using an empirical Lennard-Jones Coulomb 6-12-1 potential function.[15,16] The 3-21G* basis set geometry and partial charges obtained from a Mulliken popula-

METHYL GROUP STERIC INTERACTION IN O-XYLENE

STRUCTURE TYPE		φ (DEGREES)[a]
	A1	0.404
	A2	3.833
	B	1.813
	C	2.191
	D	1.691

[a]3-21G* BASIS SET

FIG. 3. The methyl groups effective separation φ is shown for the structures of Fig. 1 as determined from *ab initio* calculations.

TABLE III. *O*-xylene methyl group interaction energy for pairwise Lennard-Jones charge (6-12-1) potential (in cm^{-1}).[a]

	Structure	V_6	V_{12}	V_1	$V_{Relative}$
A1		−716.6	1444.4	516.5	0.0
A2		−774.0	2691.6	528.9	1202.2
B		−718.0	1628.0	452.4	118.1
C		−743.4	2026.0	519.9	558.1
D		−715.7	1604.9	450.6	95.5

[a]The dispersion and repulsion constants from Ref. 16.

TABLE IV. *Ab initio* zero point energies (ZPE) (in cm^{-1}) (3-21G* basis set) for A1.

	Structure	S_0 ZPE	S_0^- ΔZPE	Observed $S_1 \leftarrow S_0$ ΔΔZPE
d_0		36 868.55	0.0	0.0
d_1		36 109.83	−758.72 (0.0)	4.6 (0.0)
		36 120.37	−748.18 (−10.54)	13.2 (8.6)
$d_2(a)$		35 354.27	−1514.28 (0.0)	17.0 (0.0)
		35 363.84	−1504.71 (−9.57)	27.8 (10.8)
$d_2(b)$		35 351.04	−1517.51 (0.0)	7.5 (0.0)
		35 361.58	−1507.97 (−10.54)	16.6 (9.1)
		35 372.18	−1496.37 (−21.14)	26.4 (18.9)
		35 372.11	−1496.44 (−21.07)	23.6 (16.1)

tion analysis are used in this calculation and all carbon–carbon, carbon–hydrogen, and hydrogen–hydrogen methyl interactions are evaluated. The results of these calculations are given in Table III. The Coulomb and dispersion interactions for the various structures remain roughly constant at ~500 and −720 cm^{-1}, respectively; however, the short-range repulsive interactions vary by hundreds of wave numbers between the different structures and indeed correlate well with the *ab initio* calculated minimum energies for the different structures. This result is consistent with the notion that repulsions ("steric effects") contribute significantly to the intramolecular interaction responsible for the orientation of the methyl groups.

Within the Born–Oppenheimer approximation, these isotopically substituted *o*-xylenes all have the same electronic potential energy surface $E(\mathbf{R})$ upon which the nuclei move. If this surface remains unchanged upon deuteration, it should reproduce the zero point energy differences for the different isotopomers of *o*-xylene. If both S_0 and S_1 surfaces can be obtained accurately and the zero point energy (ZPE) of each isotopomer can be calculated for each surface, then the spectroscopic transition differences (ΔΔZPE) depicted in Fig. 2 should be reproduced. At present, we can only generate an accurate potential surface for S_0 and can thus only infer these spectroscopic data in a qualitative manner.

Calculations of the S_0 zero point energies for the minimum energy geometry A1 of the various isotopologues of *o*-xylene are present in Table IV. These calculations are carried out using the 3-21G* optimized geometry. Column 2 of this table lists the calculated S_0 zero point energies (ZPE). Column 3 of Table IV shows the difference between the undeuterated ZPE and the various ZPEs obtained upon deuteration (the numbers in parentheses are obtained by arbitrarily setting the lowest energy isotopomer for a specific deuteration type equal to zero). The replacement of a hydrogen atom by a deuterium atom reduces the ZPE by approximately 750 cm^{-1} per H/D exchange. The final column of Table IV lists the experimentally observed conformer features relative to the d_0 origin.

The S_0 ΔZPE values for the different isotopomers of a given mass listed in Table IV vary up to 20 cm^{-1}. The clear trend from the calculations shows consistently that

the larger zero point energy decrease upon isotopic substitution results in the smaller blue shift for the observed spectrum. This trend is, of course, opposite to that predicted based on the typical vibrational energy decrease upon $S_1 \leftarrow S_0$ excitation. The association of larger spectroscopic blue shifts for 0_0^0 transitions with larger decreases in S_0 zero point energy arises from the assumed tighter binding/steeper potential surface of the ground state with respect to that of the excited state. The observed effect is apparently more complex and subtle since the opposite trend is consistently observed. Clearly, the S_1 potential surface must be calculated and explored in a similar fashion before agreement or disagreement with experiment can be established. Note, however, that the overall trends in these RHF 3-21G* calculations are systematic; similar calculations using the semiempirical MOPAC 6 programs give basically random isotopic effects.

A comparison of the calculated normal mode energies for the A1 structure reveals that some frequencies increase while others decrease with no recognizable pattern. A more complicated view of what deuteration actually entails in this site specific instance must be taken as isotopic substitution changes not only in the reduced mass of a normal mode, but also in the mixing patterns of the various "local" modes.

TABLE V. Ground and excited state *ab initio* calculation results (in atomic units).[a]

	RHF optimized geometry	State optimized geometry[b]
RHF energy	$-308.690\ 545$	
RHF $+ 1$ cation	$-308.402\ 015$	
CASSCF results		
First root A_1 symmetry	$-308.766\ 135$	$-308.766\ 719$
Second root A_1 symmetry	$-308.582\ 149$	$-308.594\ 889$
First root B_1 symmetry	$-308.468\ 581$	

[a]One atomic unit $= 2.195 \times 10^5$ cm^{-1}.
[b]Gradients reduced to less that 10^{-5} hartree/bohr.

C. Electronic structure calculations of S_0 and S_1

To understand in more detail the nature of the S_0 and S_1 electronic states probed by the MRES experimental technique, a series of *ab initio* calculations were performed to determine excited state symmetry, excitation and ionization energies, and geometric structure. To carry out such calculations, the HONDO 8 molecular orbital package is employed.[17] The results presented here are obtained using the Dunning–Huzinaga $(9s,5p)/(3s,2p)$ contracted double zeta valence basis set. Attention is focused on the lowest energy structure A1 which possesses C_{2V} symmetry. Initially, an RHF geometry optimization is performed with energy gradients reduced to less than 10^{-5} hartree/bohr. The resulting molecular orbitals are then used in a complete active space, self-consistent field (CASSCF) calculation at the RHF geometry. The six benzene-like π orbitals included in the active space are $(b_2)^2$, $(a_2)^2$, $(b_2)^2$, (b_2), (a_2), and (a_2). Excitations within this active space result in 92 configurations for roots of A_1 symmetry and 83 configurations for roots of B_1 symmetry. Table V lists the results of these calculations. The two columns in this table correspond to calculations carried out at the RHF optimized geometry and calculations in which the geometry is optimized at the CASSCF level. The first excited singlet state clearly has A_1 symmetry and not B_1 symmetry. The estimated $1A_1$–$2A_1$ transition energy with and without geometry optimization is 40 385 and 37 717 cm^{-1}, respectively, both of which are in very good agreement with the observed value of 37 313 cm^{-1}. Geometry relaxation improves the calculated transition energy as one would expect; however, whether or not this is a fortuitous result can only be addressed by a larger calculation (improved basis set and/or increased configuration interaction). The ground $1A_1$ electronic state is comprised mainly of a single configuration $[(b_2)^2(a_2)^2(b_2)^2(b_2)(a_2)(a_2)]$ (87%), whereas the $2A_1$ excited state consists primarily of two main configurations $[(b_2)^2(a_2)^2(b_2)^1(b_2)^1(a_2)(a_2)]$ (40%) and $[(b_2)^2(a_2)^1(b_2)^2(b_2)(a_2)^1(a_2)]$ (40%), plus numerous contributions from other electronic configurations. The $1A_1$ and $2A_1$ optimized geometries are essentially identical. The ionization energy at the RHF level is calculated to be 63 332 cm^{-1} consistent with our experimental results (i.e., less than $2 \times 37\ 313$ cm^{-1}).

IV. CONCLUSIONS

The combined approach of supersonic jet mass resolved excitation spectroscopy with selective isotopic substitution can be used to elucidate detailed molecular symmetry and conformational preference information. In conjunction with *ab initio* Hartree–Fock calculations, an unambiguous description of both ground and excited state geometric and electronic state structures is achieved.

In this work, mass resolved excitation spectroscopy of partially deuterated *o*-xylenes is used to establish A1 or A2 as the minimum energy structure in both the S_0 and S_1 electronic states. *Ab initio* HF calculations using minimal and split-valence basis sets give consistent results and identify structure A1 as the lowest energy structure. This basis-set consistency is not surprising for molecules comprised exclusively of carbon and hydrogen.[18] The lowest energy *o*-xylene conformer has the smallest calculated deviation from 120° for the $\varphi(C_{ortho}$–C_{ipso}–$C_\alpha)$ bond angle. Based on HF calculated geometries together with a Lennard-Jones–Coulomb interaction potential function, a short-range steric repulsive interaction is suggested to be the major factor in defining the minimum energy structure. In addition, the multiple origin features associated with isotopomers of different mass may be used to extract potential energy surface information when combined with *ab initio* calculations. A quantitative understanding of the spectroscopic shifts for each conformer of deuterated *o*-xylenes must arise from potential surface calculations of both S_1 and S_0 states.

We are at present pursuing S_1 potential surface calculations for the *o*-xylene isotopomers. Similar studies are underway for substituted anilines, pyrazines, pyridines, and other systems.

[1]J. I. Seeman, H. V. Secor, H. S. Im, and E. R. Bernstein, J. Am. Chem. Soc. **112**, 7073 (1990).

[2](a) P. J. Breen, J. A. Warren, and E. R. Bernstein, J. Chem. Phys. **87**, 1917 (1987); (b) P. J. Breen, E. R. Bernstein, and J. I. Seeman, *ibid.* **87**, 3269 (1987); (c) P. J. Breen, J. A. Warren, E. R. Bernstein, and J. I. Seeman, J. Am. Chem. Soc. **109**, 3453 (1987); (d) P. J. Breen, E. R. Bernstein, and J. I. Seeman, J. Chem. Soc. Chem. Commun. **1988**, 393; (e) J. I. Seeman, V. H. Grassian, and E. R. Bernstein, J. Am. Chem. Soc. **110**, 8542 (1988); (f) J. I. Seeman, H. V. Secor, P. J. Breen, and E. R. Bernstein, J. Chem. Soc. Chem. Commun. **88**, 393 (1988); (g) P. J. Breen, E. R. Bernstein, H. V. Secor, and J. I. Seeman, J. Am. Chem. Soc. **111**, 1958 (1989); (h) V. H. Grassian, E. R. Bernstein, H. V. Secor, and J. I. Seeman, J. Phys. Chem. **93**, 3470 (1989); (i) J. I. Seeman, H. V. Secor, P. J. Breen, V. H. Grassian, and E. R. Bernstein, J. Am. Chem. Soc. **111**, 3140 (1989); (j) P. J. Breen, E. R. Bernstein, J. I. Seeman, and H. V. Secor, J. Phys. Chem. **93**, 6731 (1989); (k) V. H. Grassian, E. R. Bernstein, H. V. Secor, and J. I. Seeman, *ibid.* **94**, 6691 (1990); (l) H. V. Secor, J. I. Seeman, H.-S. Im, and E. R. Bernstein, J. Chem. Soc. Chem. Commun. **1990**, 87; (m) H.-S. Im, E. R. Bernstein, J. I. Seeman, and H. V. Secor, J. Am. Chem. Soc. **113**, 4422 (1991); (n) S. Li and E. R. Bernstein, Tetrahedron Lett. **32**, 3945 (1991); (o) J. I. Seeman, J. B. Paine III, H. V. Secor, H.-S. Im, and E. R. Bernstein, J. Am. Chem. Soc. (to be published); (p) J. I. Seeman, E. R. Bernstein, H.-S. Im, M. A. Young, and H. V. Secor, J. Org. Chem.

56, 6059 (1991); (q) R. Disselkamp, H.-S. Im, E. R. Bernstein, and J. I. Seeman, J. Am. Chem. Soc. (to be published).

[3] C. A. Wulff, J. Chem. Phys. **39**, 1227 (1963).

[4] J. J. Rush, J. Chem. Phys. **47**, 3936 (1967).

[5] J. Haupt and W. Muller-Warmuth, Z. Naturforsch. Teil A **23**, 208 (1968).

[6] K. F. Kuhlmann and D. M. Grant, J. Chem. Phys. **55**, 2998 (1971).

[7] R. C. Livingston, D. M. Grant, R. J. Pugmire, K. A. Strong, and R. M. Bruger, J. Chem. Phys. **58**, 1438 (1973).

[8] H. D. Rudolph, K. Walzer, and I. Krutzik, J. Mol. Spectrosc. **47**, 314 (1973).

[9] K. S. Pitzer and W. D. Gwinn, J. Chem. Phys. **10**, 428 (1942).

[10] K. C. Ingham and S. J. Strickler, J. Chem. Phys. **53**, 4313 (1970).

[11] K. M. Gough, B. R. Henry, and T. A. Wildman, J. Mol. Struct. **124**, 71 (1985).

[12] E. R. Bernstein, K. Law, and M. Schauer, J. Chem. Phys. **80**, 207 (1984).

[13] K. H. J. Ling and R. P. Hanzlik, Biochem. Biog. Res. Commun. **160**, 844 (1989).

[14] M. J. Frisch, M. Head-Gordon, H. B. Schlegel, K. Raghavachari, J. S. Binkley, C. Gonzalez, D. J. Defrees, D. J. Fox, R. A. Whiteside, R. Seeger, C. F. Melius, J. Baker, R. L. Martin, L. R. Kahn, J. J. P. Stewart, E. M. Fluder, S. Topiol, and J. A. Pople, GAUSSIAN 88 (Carnegie–Mellon Quantum Chemistry, Pittsburgh, 1989).

[15] G. Nemethy, M. S. Pottle, and H. A. Sheraga, J. Phys. Chem. **87**, 1883 (1983).

[16] F. A. Momany, R. F. McGuire, A. W. Burgess, and H. A. Sheraga, J. Phys. Chem. **79**, 2361 (1975).

[17] HONDO 8, Michel Dupuis, Abbas Farazdel, IBM Corp., Center for Scientific & Engineering Computations, Kingston, NY, 1990.

[18] W. J. Hehre and L. Radom, in *Ab Initio Molecular Orbital Theory*, edited by P. v. R. Schleyer and J. A. Pople (Wiley, New York, 1986).